www.rericjournal.ait.ac.th

Combustion Characteristics of a Methyl Ester of Pumpkin Oil in a Single Cylinder Air Cooled and Direct Injection Diesel Engine

P. Chandrasekar*, R. Prakash* and S. Murugan*[1]

Abstract *– Biodiesel is a promising alternative fuel for compression ignition engines (CI) since it has properties similar to diesel fuel. Pumpkin seed has considerable oil content. The oil from pumpkin seed can be converted into methyl ester (biodiesel) and used as an alternative fuel for CI engines. In this study, the combustion characteristics of a diesel engine fueled with methyl ester of pumpkin oil (POME) and its diesel blends (10%, 20%, 30%, 40% and 50% by volume basis) were evaluated and compared with diesel fuel. Tests were performed at different loads condition in a single cylinder, four stroke and air cooled direct injection diesel engine developing power of 4.4 kW at rated speed of 1500 rpm. From the results, it is found that the ignition delay and combustion duration are shorter for POME and its diesel blends compared to those of diesel fuel at full load condition. The maximum heat release rate occurs for diesel fuel and followed by POME diesel blends and POME. The combustion characteristics of POME and its diesel blends closely followed the diesel fuel operation. The analysis of results are presented in this paper.*

Keywords – Combustion characteristics, diesel, diesel engine, pumpkin oil methyl ester.

1. INTRODUCTION

Biodiesel is considered as one of the first generation biofuels for transportation. It can be produced from biomass materials such as vegetable oils, animal fats and algae by transesterification process. Biodiesel is a multi-component fuel that consists of monoalkyl ester of long-chain fatty acids derived from vegetable oils and animal fats [1], [2]. Biodiesel is mainly composed of five saturated and unsaturated methyl esters, such as methyl palmitate, methyl stearate, methyl oleate, methyl linoleate, and methyl linolenate [3]. The oxygen content in biodiesel changes combustion phase and partially contributes to 9% less heating of biodiesel compared to conventional diesel fuel [4]. The physical properties of biodiesel (*e.g.*, surface tension and kinematic viscosity) are much different from those of conventional diesel fuel [5], [6]. It is reported that the differences in physical properties of biodiesel make differences in atomization characteristics of fuel sprays [7], [8]. Therefore, combustion and emission characteristics of biodiesel fuel are significantly different from those of conventional diesel fuel. Reports on the use of biodiesel in diesel engines indicate a substantial reduction in SO_2, CO, and polycyclic aromatic hydrocarbons (PAHs). Higher the percentage of biodiesel in the blend, higher the reduction in the emissions. The comparison of previously documented research works on the study of combustion characteristics of diesel engine fueled with methyl esters of different edible oils in comparison with diesel fuel at full load condition are given in Table 1.

Pumpkin seed oil is an edible oil, which is used in little quantities for medicinal purpose and locally made sweets in India. The main cultivation of pumpkin seed areas are South and East Austria and neighboring countries, southern parts of North America and Central America, some regions in Africa as well as Asia [16]. In India, the pumpkin seed oil is produced in a batch process in small mills that are located in villages. The pumpkin seed oil (PSO) is dark green colour and viscous [17]. The oil content of the pumpkin seed varies from 42–54% and the composition of free fatty acids (FFA) is dependent on several factors (variety, area in which the plants are grown, climate, state of ripeness). The dominant FFA comprise palmitic acid (C16:0, 9.5–14.5%), stearic acid (C18:0, 3.1–7.4%), oleic acid (C18:1, 21.0–46.9%) and linoleic acid (C18:2, 35.6–60.8%). These four FFA make up 98±0.13% of the total. Other FFA is well below 0.5% [18]. Table 2 shows the fatty acid composition of PSO.

As the FFA content of refined oil is less than 3%, it can be easily converted into biodiesel by base catalyzed reaction alone [20], [21]. For vegetable oils with high FFA content, the base catalyst reaction is not suitable for transesterification [22], [23]. Moreover, pumpkin seed is a rich source for medical applications and includes various bioactive compounds such as ω–3, ω–6 and ω–9 fatty acids, α–tocopherols and γ–tocopherols, Δ5–sterols and Δ7–sterols, β–carotene and lutein [24]- [27]. A two-step transesterification process (acid catalyzed followed by base catalyzed) is required to convert a high FFA pumpkin oil into methyl ester.

2. MATERIALS USED AND EXPERIMENTATION

2.1 Production of Pumpkin Oil Methyl Ester

The two major quality parameters that influence the production process of biodiesel are FFAs and water content. Production of biodiesel from pumpkin oil by using transesterification method was done by adding 18 grams of KOH and 200 ml of MeOH with 1 litre of pumpkin oil. The schematic diagram of the complete oil

*Department of Mechanical Engineering, National Institute of Technology, Rourkela, Orissa – 769008, India.

[1]Corresponding author; Tel: + 919437140949.
E-mail: recmurugan@yahoo.co.in.

extraction and oil transesterification process flow diagram is shown in Figure 1. A comparison of the physical and chemical properties of the PSO, POME and diesel is shown in Table 3.

Table 1. Combustion characteristics of diesel engine fueled with methyl esters of different edible oils.

Combustion parameters	Sunflower	Soya bean	Palm oil	Rice bran	Coconut	Rapeseed
Cylinder peak pressure	↓	↑	↓	↑	↓	↓
Ignition delay	↓	↓	↓	↓	↓	↓
Maximum heat release rate	↓	↓	↓	↑	↓	↓
Combustion duration	NA	↓	↓	↓	NA	↓
Mass fraction burned	NA	↑	↓	↓	NA	NA
Rate of pressure rise	↓	↑	NA	↓	NA	↓
Test engine	Mercedes-Benz, Six-cylinder, In-line engine	Single cylinder 4-Stroke, DI, diesel engine	Kirloskar TV-1, Single cylinder, 4 Stroke diesel engine	Four cylinder Four-stroke, NA, Water cooled diesel engine	Lister-Petter AD1, Single cylinder diesel engine	John Deere 4276T, four-cylinder, four-stroke, turbocharged DI diesel engine
Source	[9]	[10,11]	[12]	[13]	[14]	[15]

Table 2. Fatty acid composition of pumpkin oil [19].

Fatty acid	Structure	Formula	Composition % weight
Palmitic	C16:0	$C_{16}H_{32}O_2$	12.51
Stearic	C18:0	$C_{18}H_{36}O_2$	5.43
Oleic	C18:1	$C_{18}H_{34}O_2$	37.07
Linoleic	C18:2	$C_{18}H_{32}O_2$	43.72
Linolenic	C18:3	$C_{18}H_{30}O_2$	0.18
Lignoceric	C24:0	$C_{24}H_{48}O_2$	0.06

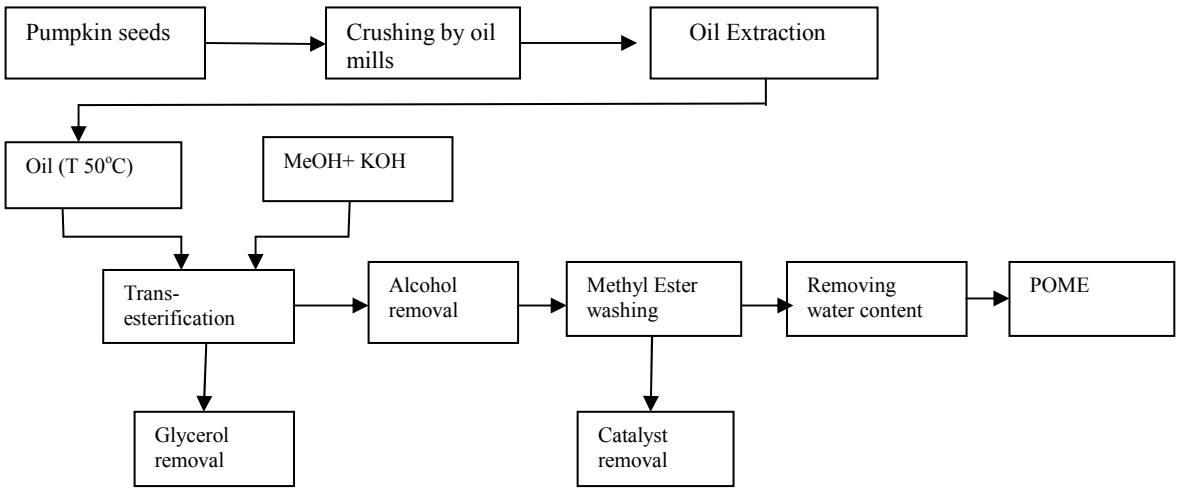

Fig. 1. Pumpkin oil extraction and transesterification process flow diagram

Table 3. Physical and chemical properties.

Property	Diesel	PSO	POME
Kinematic viscosity (40°C), mm^2/sec	3–5	35.6	4.41
Density (15°C), kg/m^3	860	921.6	883.7
Flash point, °C	45–76	>230	>120
Sulphur content, µg/g	0.05	2	2
Water content, µg/g	–	584	490
Iodine number	–	115	115
Net calorific value MJ/kg	44.8	35.1	34.27
Cetane number	40–55	52.6*	59.8*

* calculated cetane number

It is understood from the available literature that no information is available on the combustion behavior of pumpkin seed oil and pumpkin oil methyl ester blends. Therefore the proposed research work is aimed to study the combustion characteristics of the pumpkin oil methyl ester blends as fuels in a single cylinder, four stroke, direct injection diesel engine and presented in this paper.

In the present study the POME and its diesel blends varying from 10% to 50% at a regular interval of 10% on volume basis were used as fuels in a single cylinder, four strokeS, air cooled, direct injection diesel engine. The blends are denoted as POME followed by the percentage of methyl ester (*i.e.*, POME 10 indicates 10% methyl ester of pumpkin oil and 90% diesel). The combustion parameters were evaluated compared, with normal diesel fuel operation and presented in this paper.

2.2 Experimental Procedure

Figure 2 shows the schematic arrangement of the experimental setup. The engine used in this investigation is a stationary diesel engine, which is usually used for agricultural and low power generation purposes. The technical specifications of the engine are given in Table 4. A load cell was fitted with an electrical dynamometer (alternator) to provide the load to the engine. The data-acquisition system consisted of a Kistler piezoelectric pressure transducer model: 5395A, a charge amplifier, a computer and a crank angle encoder. Fuel consumption was measured with the help of a solenoid controlled automatic burette. Air consumption was measured by a differential pressure sensor fitted in the air box.

A surge tank was used to damp out the pulsations produced by the engine, for ensuring a steady flow of air through the intake manifold. A non contact type sensor was connected near the flywheel of engine to measure the speed. Twenty three channel signal analyzer was used for data acquisition and the acquired data was transferred through ethernet cable and stored in a personal computer for offline analysis. A continuous circulation of air is maintained for cooling the transducer, by using fins to maintain the required temperature. A crank position sensor is connected to the output shaft to record the crank angle. Combustion parameters such as the peak pressure, time of occurrence of peak pressure, heat release rate and ignition delay are obtained with the help of software.

Table 4. Specifications of engine.

Make	Kirloskar
Model	TAF 1
Bore x Stroke	87.5 x 110 mm
Compression ratio	17.5:1
Piston type	Bowl-in-piston
Number of valves	2
Rated power	4.4 kW
Rated speed	1500 rpm
Type of fuel injection	Pump-line-nozzle injection system
Nozzle type	Multi hole
No. of holes	3
Start of injection	23° bTDC
Nozzle opening pressure	200 bar

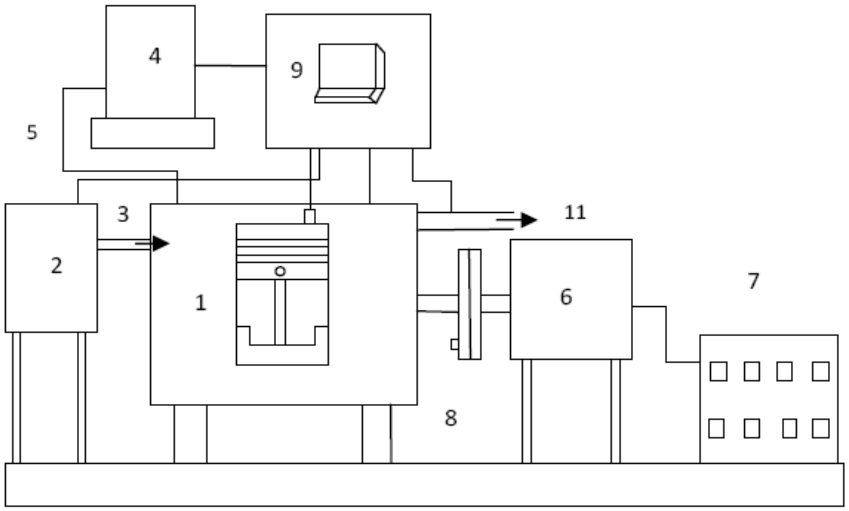

1.Diesel engine 2. Air tank 3. Air flow sensor 4.Fuel tank
5. Fuel sensor 6. Dynamometer 7. Load cell 8. CA encoder
9.DAQ 10.Pressure transducer 11. Exhaust

Fig. 2. Schematic arrangement of the experimental setup.

2.3 Error Analysis

An uncertainty analysis was performed using the method described by Holman [28]. Table 5 shows the instruments used in the present study and their uncertainties.The total percentage of the uncertainty of this experiment is calculated as given below:

$= [(\text{Total fuel consumption})^2 + (\text{Brake power})^2 + (\text{brake specific fuel consumption})^2 + (\text{speed})^2 + (\text{pressure pick up})^2 + (\text{crank angle encoder})^2]^{1/2}$

$= [\{(1.5)^2 + (0.2)^2 + (1.5)^2 + (0.1)^2 + (0.15)^2 + (1)^2]^{1/2}$

$= \pm 2.36\ \%$

All the tests were conducted by starting the engine with diesel only. After the engine was warmed up, it was switched to the respective POME and its diesel blends operation. At the end of the test, the fuel was switched back to diesel and the engine was kept running for a while, before shut-down to flush the POME base fuels from the fuel line and the injection system.

3. RESULTS AND DISCUSSION

3.1 Pressure – Crank Angle History

In a compression ignition engine, the peak cylinder pressure depends on the burned fuel fraction during the premixed burning phase, *i.e.* the initial stage of combustion. The cylinder pressure is characterized by the ability of the fuel to mix well with air and burn. The pressure variation with crank angle as shown in Figure 3, for diesel, POME and its diesel blends.

It is observed that the peak pressure of biodiesel blends is higher than that of diesel fuel followed by 10%, 20%, 30%, 40% and 50%. This may be due to the ignition delay period that increases with the decrease of engine load. The diesel fuel has longer ignition delay period so, the combustion starts later for diesel fuel than biodiesel blends [11]. For POME, the cylinder pressure is lower than diesel, due to higher viscosity and lower volatility of biodiesel [29].

3.2 Ignition Delay

Ignition delay is defined as the time difference in crank angle between start of injection and start of combustion. The value of ignition delay helps to determine the heat release, maximum pressure and rate of pressure rise *etc*. The ignition delay is calculated [30] by the following Equation 1.

$$ID = 3.45\ exp^{\left(\frac{2100}{T_m}\right)} p_m^{-1.02} \quad (1)$$

Where, T_m and p_m are the mean temperature and pressure of the ambient during ignition delay respectively. The variation of ignition delay with brake power for diesel, POME and its diesel blends is shown in Figure 4.

The ignition delay decreases with increase in load as a result of higher combustion chamber wall temperature at the time of injection and reduced exhaust gas dilution [31]. It is observed that the ignition delay for POME and its diesel blends is shorter than that of diesel and decrease with increase in percentage of POME in the blend. This may be due to higher cetane number of POME and its diesel blends compared to that of diesel [32]. At full load condition, the ignition delay period of diesel, 10%, 20%, 30%, 40%, 50% and POME are 11.45°CA, 11°CA, 10.71°CA, 11°CA, 11°CA, 10.714°CA and 10.13 °CA, respectively.

Table 5. Accuracy and uncertainty of the instruments

Instrument	Accuracy	Uncertainty
Load indicator	±10W	0.2
Temperature indicator	±1 °C	0.1
Burette	±0.2 cc	1.0
Speed sensor	±10rpm	0.1
Pressure transducer	±0.1bar	0.15
Crank angle encoder	±0.2°	0.5

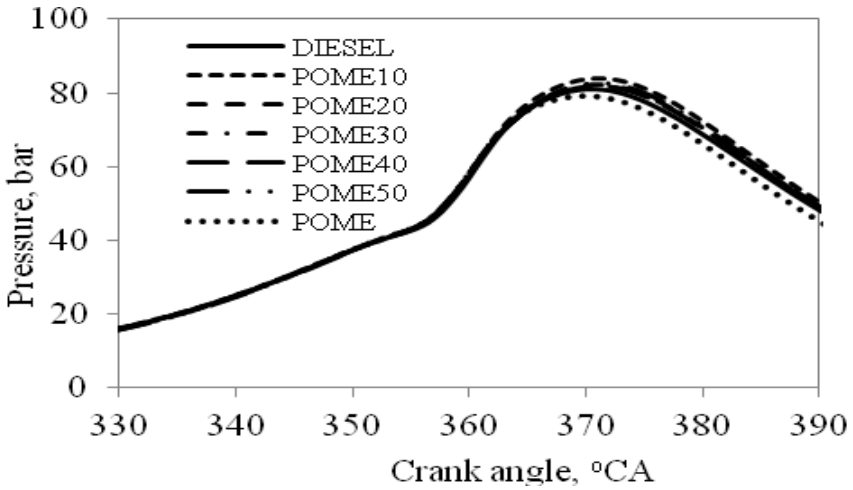

Fig. 3. Variation of cylinder pressure with crank angle.

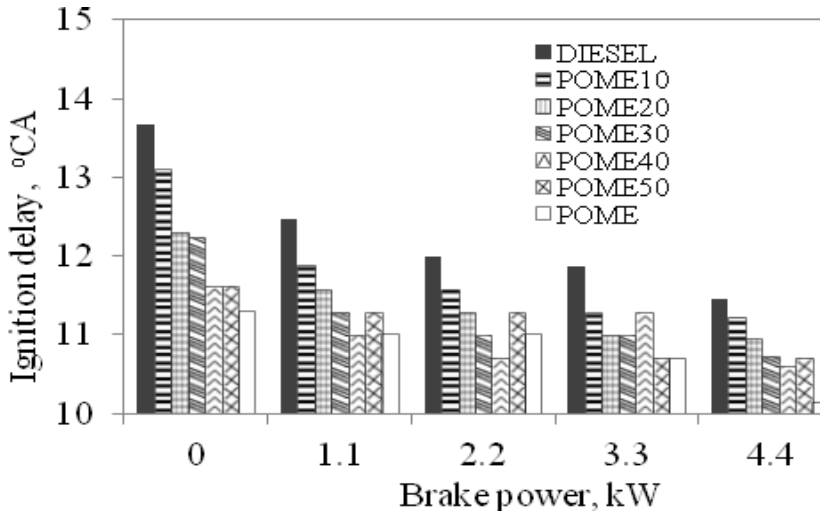

Fig. 4. Variation of ignition delay with brake power.

3.3 Heat Release Rate

A thermodynamic model based on first law is used to determine the heat release rate. The model assumes thermodynamic equilibrium during combustion in the cylinder, but eliminates temperature gradients, pressure waves, non-equilibrium conditions, fuel vaporization, mixing and *etc.* [33].

From the first law of thermodynamics:

$$\frac{dU}{dt} = \dot{Q} - \dot{W} \quad (2)$$

$$mC_v\frac{dT}{dt} = \dot{Q} - P\frac{dv}{dt} \quad (3)$$

Where, $\dot{Q}$= the combination of the heat release rate and the heat transfer rate across the cylinder wall,

$\dot{W}$ = the rate of work done by the system due to system boundary displacement.

To simplify Equation 3 the ideal gas assumption can be used.

$$PV = mRT \quad (4)$$

Equation 4 can be differentiated (assuming constant mass)

$$\frac{dT}{dt} = \frac{1}{mR}\left[P\frac{dV}{dt} + V\frac{dP}{dt}\right] \quad (5)$$

After combining these two equations, the heat release equation becomes

$$\dot{Q} = \left[\frac{Cv}{R} + 1\right]P\frac{dV}{dt} + \frac{Cv}{R}V\frac{dP}{dt} \quad (6)$$

After replacing time (t) with the crank angle (h), the equation becomes

$$\dot{Q} = \frac{\lambda}{\lambda - 1}P\frac{dV}{d\theta} + \frac{1}{\lambda - 1}V\frac{dP}{d\theta} \quad (7)$$

Where, k = the ratio of specific heats, C_p/C_v. For diesel heat release analysis, λ is 1.35 [34].

The comparison of heat release rate of POME and its diesel blends with diesel is shown in Figure 5. Due to heat loss from the cylinder and the cooling effect of the fuel vaporizing as it is injected into the cylinder, the heat release rate is slightly negative during the ignition delay period [35]. It can be observed that the heat release rate of 10% blend is higher than that of diesel but other diesel blends (20%, 30%, 40% and 50%) and POME is lower than that of diesel, which may be attributed to the lower calorific value of the blends and POME than that of diesel fuel [36]. A higher rate of heat release occurs at POME10 diesel blend may be the reason of higher boiling point [37].

At the time of ignition, less fuel/air mixture is prepared for combustion with the diesel blends; therefore, more burning occurs in the diffusion-burning phase rather than in the premixed phase [31]. It is observed that the maximum heat release rate of 56.41 J/ ^{o}CA is recorded for diesel at 4^{o}aTDC, while POME records its maximum heat release rate of 53.705 J/^{o}CA.

3.4 Combustion Duration

The variation of the total duration of combustion with brake power for different fuels is shown in Figure 6. This time duration accounts from the beginning of the heat release to the end of heat release [38]. It can be observed that the total duration of combustion is shorter for POME and its diesel blends while comparing with diesel fuel. Higher oxygen content in the POME and its diesel blends is believed to have enhanced flame velocity that resulted in reduction of combustion duration, compared to that of diesel [36].

At full load condition, the combustion duration for diesel, POME and its diesel blends are 38.34, 35.23 and 36.93, 36.77, 36.68, 36.23, 36.6^{o}CA, respectively. The decrease in combustion duration is due to the efficient combustion of the injected fuel.

3.5 Peak Pressure

The variation of peak pressure with respect to brake power for diesel, POME and its blends is shown in Figure 7. Peak cylinder pressure is the maximum chamber pressure achieved during the combustion process.

From the results, it can be observed that the peak pressure is higher for biodiesel blends compared to those that of diesel. The high viscosity and low volatility of POME lead to poor atomization and mixture preparation with air during the ignition delay period so it recorded lower peak pressure than that of diesel at full load [39]. The peak pressures are 80.96 bar, 84.07 bar, 82.44 bar, 82.08 bar, 81.74 bar, 82.6 bar and 78.98 bar for diesel, POME blends (10%, 20%, 30%, 40%, 50%) and POME, respectively at full load. This is due to the lower ignition delay of POME and its diesel blends [40]. The oxygen content of POME, that which results in better combustion, may also result in higher peak pressure compared to diesel [31].

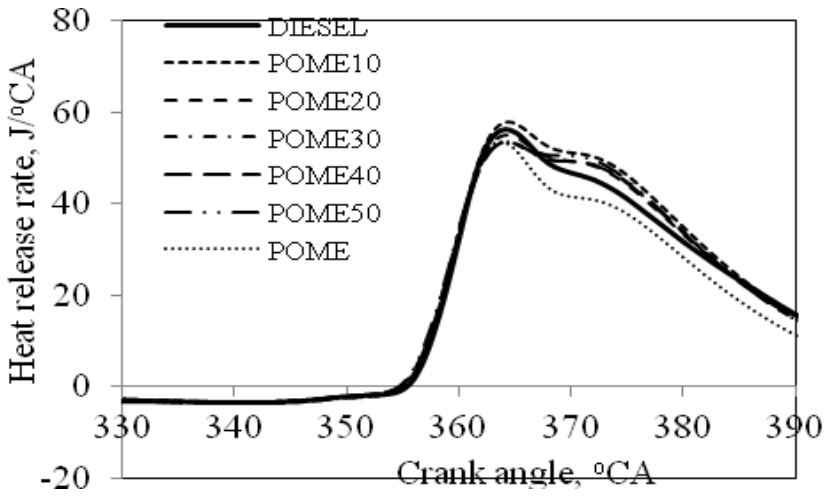

Fig. 5. Variation of heat release rate with crank angle.

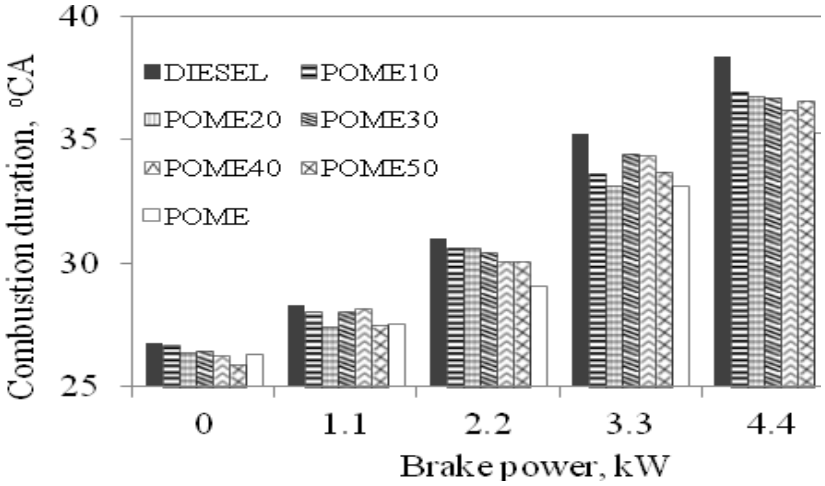

Fig. 6. Variation of combustion duration with brake power.

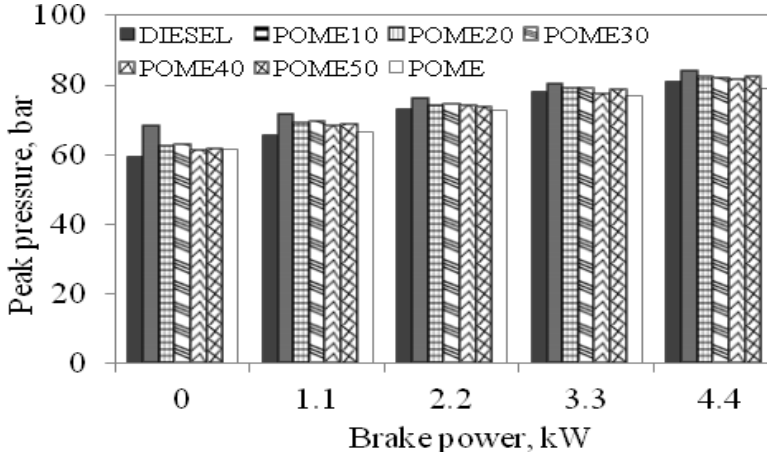

Fig. 7. Variation of peak pressure with brake power.

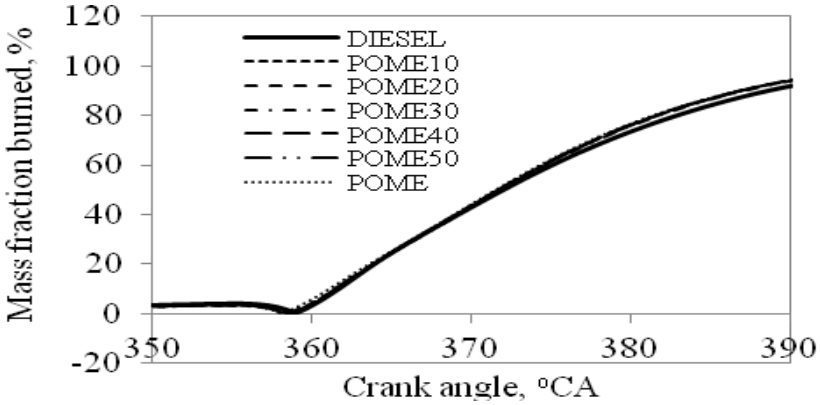

Fig. 8. Variation of mass fraction burned with crank angle at full load.

3.6 Mass Fraction Burnt

Assuming that the pressure rise Δp_c is proportional to the heat added to the in-cylinder medium during the crank angle interval, the mass fraction burned at the end of the considered i-th interval may be calculated as [34].

$$\text{MFB} = \frac{m_b\ (i)}{m_b\ (total)} = \frac{\sum_0^i \Delta p_c}{\sum_0^N \Delta p_c} \quad (8)$$

Where 0 denotes the start of combustion, N – end of combustion (N is the total number of crank intervals).

The variations of the mass fraction burnt with the crank angle for POME and its diesel blends compared with diesel at full load is given in Figure 8. The mass fraction burnt of POME and its diesel blends is slightly higher than that of diesel at full load. Due to the oxygen content of the blends and POME the combustion is sustained in the diffusive combustion phase [38]. The

90% of mass fraction burned for diesel and POME is 390.3 ^{o}CA and 388.65 ^{o}CA, respectively. The highest rate of burning shows that the efficient rate of combustion.

3.7 Rate of Pressure Rise

Rate of pressure rise is indicative of noisy operation of an engine. A value exceeding 8 bar/^{o}CA is generally considered as unacceptable for a compression ignition engine [36]. Figure 9 shows the variation of rate of pressure with crank angle at full load.

All the tests were performed at an injection timing 23^{o}bTDC. It can be observed that the rate of pressure rise for diesel is higher compared to POME and its diesel blends. This is due to longer ignition delay of diesel compared to POME and its diesel blends [40]. A comparison of combustion parameters are given in Table 6.

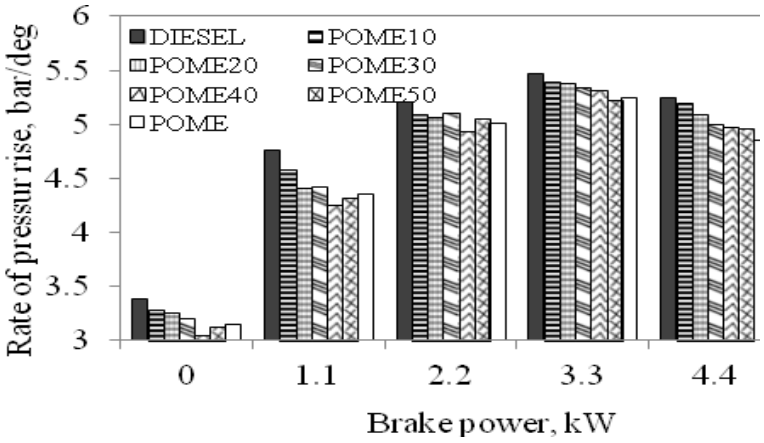

Fig. 9. Variation of rate of pressure rise with crank angle.

Table 6. Combustion parameters at full load.

Parameter	Diesel	10%	20%	30%	40%	50%	POME
Ignition delay, ^{o}CA	11	11	10.712	11	11	10.714	10.13
Cylinder pressure, bar	80.96	84.07	82.44	82.08	81.74	82.06	78.98
Heat release rate J/^{o}CA	56.41	57.91	54.93	53.05	53.38	53.71	53.7
Combustion duration, ^{o}CA	38.34	36.23	36.77	36.68	36.23	36.6	37.29
Rate of pressure rise, bar/^{o}CA	4.65	4.71	4.49	4.41	4.38	4.39	4.57

4. CONCLUSIONS

The combustion parameters such as ignition delay, peak pressure, pressure crank angle diagram, heat release rate, combustion duration, rate of pressure rise and mass fraction burned were evaluated for different engine loads at constant engine speed of 1500 rpm in a single cylinder, four stroke and air cooled direct injection diesel engine developing power of 4.4 kW. The conclusions are summarized as follows;

- From the combustion analysis, it is found that the POME40 can be considered as an optimum blend. The pressure crank angle and rate of pressure rise are comparable with standard diesel fuel.
- From the combustion analysis, the POME and its diesel blends exhibits shorter ignition delay and combustion duration than that of diesel. The ignition delay for diesel, POME and its diesel blends were shorter by about 1 – 1.5 ^{o}CA at full load.
- The rate of heat release for diesel is 56.41 J/^{o}CA. However the POME and its diesel blends are 2 – 3 J/^{o}CA lower than diesel fuel. The mass fraction burnt for POME and its diesel blends are higher than that of diesel at full load.
- However, further research and development on the additional fuel property measures, long-term run and wear analysis of biodiesel fuelled engine is also necessary along with injection timing and duration for better combustion of biodiesel in diesel engines.

NOMENCLATURE

CI	compression ignition
POME	pumpkin oil methyl ester
CO	carbon monoxide
PSO	pumpkin seed oil
SO_2	sulphur dioxide

FFA	free fatty acid
KOH	potassium hydroxide
MeOH	methanol
DAQ	data acquisition system
TDC	top dead centre
CA	crank angle
CO_2	carbon dioxide
NO	nitric oxide
ID	ignition delay
MFB	mass fraction burned

REFERENCES

[1] Demirbas A., 2003. Biodiesel fuels from vegetable oils via catalytic and non-catalytic supercritical alcohol transesterification and other methods: a survey. *Energy Conversion Management* 44:2093–109.

[2] Ma F., and M.A. Hanna. 1999. Biodiesel production: a review. *Bioresource Technology* 70:1–15.

[3] Herbinet O., Pitz W.J. and Westbrook C.K., 2008. Detailed chemical kinetic oxidation mechanism for a biodiesel surrogate. *Combustion Flame* 154: 507–528.

[4] Lee C.S., Park S.W. and Kwon S.I., 2005. An experimental study on the atomization and combustion characteristics of biodiesel-blended fuels. *Energy Fuels* 19:2201–2208.

[5] Li W., Ren Y., Wang X.B., Miao H., Jiang D.M. and Huang Z.H., 2008. Combustion characteristics of a compression ignition engine fuelled with diesel—ethanol blends. *Proceedings of the Institute of Mechanical Engineers, Part D: Journal of Automobile Engineering* 222:265–274.

[6] Fleisch T.C., McCarthy, and Basu, A., 1995. A new clean Diesel technology: demonstration of ULEV emissions on a Navistar Diesel engine fueled with dimethyl ether. *SAE Transactions* 104(4):42–53.

[7] Shiga S., Ozone S., Machacon H.T.C., Karasawa T., Nakamura H., Ueda T., Jingu N., Huang Z., Tsue M. and Kono M., 2002. A study of the combustion and emission characteristics of compressed-natural-gas direct-injection stratified combustion using a rapid-compression-machine. *Combustion Flame* 129(1-2):1–10.

[8] Sorenson S.C. and S.E. Mikkelsen. 1995. Performance and emissions of a 0.273 liter direct injection diesel engine fueled with neat dimethyl ether. *SAE Transactions* 104(4):80–90.

[9] Rakopoulos K.C., 2012. Heat release analysis of combustion in heavy-duty turbocharged diesel engine operating on blends of diesel fuel with cottonseed or sunflower oils and their bio-diesel. *Fuel* 96:524–534.

[10] Qi D.H., Geng L.M., Chen H., Bian, Z.H., Liu Y. and Ren X.C.H., 2009. Combustion and performance evaluation of a diesel engine fueled with biodiesel produced from soyabean crude oil. *Renewable Energy* 34:2706–2713.

[11] Qi D.H., Chen H., Geng L.M. and ZH.Bian Y., 2010. Experimental studies on the combustion characteristics and performance of a direct injection engine fuelled with biodiesel/diesel blends. *Energy Conversion and Management* 51:2985–2992.

[12] Sharon H., Karuppasamy K., Soban Kumar D.R. and Sundaresan A., 2012. A test on DI diesel engine fueled with methyl esters of used palm oil. *Renewable Energy* 47:160-166.

[13] Agarwal A.K. and A. Dhar. 2010. Comparative performance, emission and combustion characteristics of rice-bran oil and its biodiesel in a transportation diesel engine. *Journal of Engineering for Gas Turbines and Power* 132*(*064503):1-4.

[14] Shaheed A. and E. Swain. 1999. Combustion analysis of coconut oil and its methyl esters in a diesel engine. *Proceedings of the Institute of Mechanical Engineers, Part A* (213):417-425.

[15] Canakci M., 2007. Combustion characteristics of a turbocharged DI compression ignition engine fueled with petroleum diesel fuels and biodiesel. *Bioresource Technology* 98:1167–1175.

[16] Lankmayra E., Mocakb J., Serdtc K., Ballab B., Wenzla T., Bandonienea D., Gfrerera M. and Wagnerd S., 2004. Chemometrical classification of pumpkin seed oils using UV–Vis, NIR and FTIR spectra. *Journal of Biochemistry and Biophysics Methods* 61:95–106.

[17] Teppner H., 2000. Cucurbitapepo (Cucurbitaceae)-history, seed coat types, thin coated seeds and their genetics. *Phyton* 40:1–42.

[18] Murkovic M., Hillebrand A., Winkler J. and Pfannhauser W., 1996. Variability of vitamin E content in pumkin seeds (Cucurbitapepo L). *European Food Research and Technology* 202: 275–278.

[19] Schinas P., Karavalakis G., Davaris C., Anastopoulos G., Karonis D., Zannikos F., Stournas S. and Lois E., 2009. Pumpkin (Cucurbitapepo L.) seed oil as an alternative feed stock for the production of biodiesel in Greece. *Biomass and Bioenergy* 33:44–49.

[20] Gupta P.K., Kumar R., Panesar B.S. and Tapar V.K., 2007. Parametric studies on bio-diesel prepared from rice bran oil. *Agricultural Engineering International: The CIGR E Journal*, IX, Manuscript EE 06 007.

[21] Shailendra S., Agarwal A.K. and Sanjeev G., 2008. Biodiesel development from rice bran oil: transesterification process optimization and fuel characterization. *Energy Conversion and Management*, 49(5):1248–57.

[22] Canakci M. and J. Vangerpen. 2001. Biodiesel production from oils and fats with high free fatty acids. *Transactions of the ASAE* 46(9):1429–36.

[23] Meher L.C., Vidyasagar D. and Naik, S.N., 2006. Technical aspects of biodiesel production by

tranesterification – a review. *Renewable and Sustainable Energy Reviews* 10(3):248–68.

[24] Murkovic M., Hillebrand A., Winkler J., Leitner E. and Pfannhauser W., 1996. Variability of fatty acid content in pumpkin seeds (Cucurbitapepo L.). *European Food Research and Technology* 203:216–219.

[25] Murkovic M., Piironen V., Lampi A.M., Kraushofer T. and Sontag G., 2004. Changes in chemical composition of pumpkin seeds during roasting process for production of pumpkin seed oil (Part 1: non-volatile compounds). *Food Chemistry* 84:359–365.

[26] Nakic S.N., Rade D., Kevin D., Strucel, D., Mokrovcak Z. and Bartolic M., 2006. Chemical characteristics of oils from naked and husk seeds of Cucurbitapepo L. *European Journal of Lipid Science and Technology* 108:936–943.

[27] Fruhwirth G.O. and A. Hermetter. 2008. Production technology and characteristics of Styrian pumpkin seed oil. *European Journal of Lipid Science and Technology* 110:637–644.

[28] Holman J.P., 2003. Experimental techniques. Tata McGraw Hill Publications.

[29] Ekrem B., 2010. Effects of biodiesel on a diesel engine performance, emission and combustion characteristics. *Fuel* 89:3099–105.

[30] Watson N., Pilley A.D. and Marzouk M., 1980. A Combustion Correlation for Diesel Engine Simulation. *SAE*, 800029.

[31] Enweremadu C.C. and H.L. Rutto. 2010. Combustion, emission and engine performance characteristics of used cooking oil biodiesel - a review. *Renewable and Sustainable Energy Reviews* 14:2863–2873.

[32] Arul MozhiSelvan V., Anand R.B. and Udayakumar M., 2009. Combustion characteristics of Diesohol using bio diesel as an additive in a direct injection ignition engine under various compression ratios. *Energy and Fuels* 23:5413–22.

[33] Krieger, R.B. and G.L. Borman. 1966. The computation of applied heat release for internal combustion engines. *ASME Paper*, 66, WA/DGP–4.

[34] Heywood J.B., 1988. *Internal combustion engine fundamentals*. McGraw-Hill, New York.

[35] Sinha S. and A.K. Agarwal. 2005. Combustion characteristics of rice bran oil derived biodiesel in a transportation diesel engine. *SAE* 2005–01–1730.

[36] Pradeep V. and R.P. Sharma. 2005. Evaluation of performance, emission and combustion parameters of a CI engine fuelled with bio-diesel from rubber seed oil and its blends. *SAE* 2005–26–353.

[37] Devan P.K., and N.V. Mahalakshmi. 2009. Performance, emission and combustion characteristics of poon oil and its diesel blends in a DI diesel engine. *Fuel* 88:861–867.

[38] Muralidharan K., Vasudevan D. and Sheeba K.N., 2011. Performance, emission and combustion characteristics of biodiesel fuelled variable compression ratio engine. *Energy* 36:5385–5393.

[39] Senthil Kumar M., Ramesh A. and Nagalingam B., 2003. An experimental comparison of methods to methonal and jatropha oil in a compression ignition engine. *Biomass and Bioenergy* 25:309-318.

[40] Lakshmi, Narayana Rao G., Sampath S. and Rajagopal K., 2008. Experimental studies on the combustion and emission characteristics of a diesel engine with used cooking oil methyl ester and its diesel blends. *International Journal of Engineering and Applied Sciences* 4:2.